

Volume dependence of the long-range two-body potentials in various color channels by lattice QCD

Y. Nakagawa,¹ A. Nakamura,² T. Saito,³ and H. Toki¹

¹*Research Center for Nuclear Physics, Osaka University, Ibaraki, Osaka 567-0047, Japan*

²*Research Institute for Information Science and Education, Hiroshima University, Higashi-Hiroshima 739-8521, Japan*

³*Integrated Information Center, Kochi University, Kochi, 780-8520, Japan*

(Received 30 August 2007; published 21 February 2008)

We study the color-dependent confining forces between two quarks by the quenched lattice simulations of Coulomb gauge QCD. The color-singlet and color-antitriplet instantaneous potentials yield attractive forces. The ratio of the string tensions obtained from them is approximately 2, and these tensions have little volume dependence. Meanwhile, the color-octet and color-sextet channels give a minor contribution to the two-quark system. We finally find that the infrared self-energy of the color-nonsinglet channels diverges in the infinite volume limit; however, the degree of the divergence on the finite lattice can be understood in terms of color factors.

DOI: [10.1103/PhysRevD.77.034015](https://doi.org/10.1103/PhysRevD.77.034015)

PACS numbers: 12.39.Mk, 11.15.Ha, 12.38.Aw, 12.38.Gc

I. INTRODUCTION

The long-distance color-dependent forces among quarks and gluons are the key quantities for the understanding of the internal structure of the hadron as well as color-confinement dynamics. The quarks and gluons are described in quantum chromodynamics (QCD), and they have a color charge based on the $SU(3)$ group, with which the quark combination yields many color-dependent forces including both attractive and repulsive forces. They make the hadron structure (quark bound state) more complicated. Therefore, it is essential to know the basic behavior of the color-dependent force at short and long distances.

The color-dependent force will be important when one investigates the multi-quark hadron (made of more than four quarks) and the exotic meson, etc. Although many candidates of those particles have been recently reported by experimental groups [1,2], it is still a hard task to theoretically understand those new particles. They may consist of many quarks with various color-dependent forces that make their internal structure more complicated than the existing baryons. The quark interaction at short distances can be characterized by a coefficient $\langle \lambda \cdot \lambda \rangle$ of a one-gluon-exchange potential. This is a basic assumption if we construct a quark model to deal with the baryon system. However, owing to the quark confinement, it is not obvious how quarks behave for large quark separation. We thus need a lattice simulation to obtain a nonperturbative feature for the long-range color-dependent force.

However, the lattice study along this line is sparse, although there are many lattice studies about the $q\bar{q}$ potential [3] obtained by the gauge-invariant Wilson-loop operator. This operator mixes color-singlet with color-octet contributions; therefore, we cannot separately extract the color-octet potential from the Wilson loop. In spite of this, the color-octet process has been discussed in the detailed analysis of the J/ψ photoproduction to explain the deviation between the experimental data and the theoretical

predictions [4–6]. On the other hand, there is no lattice calculation for the qq sector as well; however, the diquark (color- $3^* qq$) is also an important ingredient in hadron physics. The existence of the diquark has been believed by many physicists and applied to work out unsolved problems [7–12]. Note that the qq potential in the lattice theory is not formulated gauge invariantly.

In this study, we employ a color-dependent Polyakov line correlator (PLC) with the Coulomb gauge fixing in order to clarify the color-dependent forces [13,14]. In the quark-gluon plasma phase, there have already been some numerical studies of the color-screened color-dependent force with the Coulomb and Landau gauge fixings [15–18]. Investigating the confining color-dependent forces, we use Coulomb gauge QCD [19], the theoretical background of which has recently been well studied [19–21]. In this theory, the PLC potential can be separated into the vacuum polarization part and the color-Coulomb instantaneous part; the latter relatively produces a clear numerical signal, even in the confinement phase [22–25]. The color-Coulomb instantaneous potential is not the same as the Wilson-loop potential. However, it yields an upper bound of a linearly rising quark potential [26] and is the most important quantity on the Coulomb gauge confinement scenario [19]. The infrared singularity of this potential is caused by accumulation of the Faddeev-Popov ghost eigenvalue at the vanishing momentum [27,28].

Coulomb gauge QCD may provide the most favorable framework when one considers the hadron phenomenological studies such as the constituent quark model. The Coulomb gauge as a physical gauge gives a positive-definite Fock space that is suitable for constructing effective Hamiltonians. Moreover, the color-Coulomb instantaneous potential without the vacuum polarization (or a retarded effect) is required to make a quark bound state in analogy with quantum electrodynamics (QED). This formulation is applicable in the heavy-quark system with

no retarded effect, as well as in the light-quark system with constituent quarks due to chiral-symmetry breaking [29].

In this paper, we study the long-distance divergence behavior of the color-dependent forces. Because the color-nonsinglet state cannot exist in nature, singularities in such states will emerge on the lattice as a finite-volume effect. This has not been verified in the previous calculation [13], and thus we should investigate their divergence behavior on a variety of lattice sizes. We also discuss the color-factor dependence for the degree of the divergence and will confirm this point by the numerical lattice simulation. In Sec. II, we briefly summarize Coulomb gauge QCD and the definition of the color-dependent potentials with the PLCs. In Sec. III, we give lattice numerical results and fitting analyses. Section IV is devoted to our summary.

II. COLOR-DEPENDENT POTENTIALS

A. Instantaneous potential in Coulomb gauge QCD

Coulomb gauge QCD has been quantized through the Faddeev-Popov technique [19], and renormalizability of this theory has also been proved in terms of the Hamiltonian and Lagrangian formalism [20,21]. The use of Coulomb gauge as a physical gauge leads us to classify transverse gluon modes and an instantaneous interaction, which is required to make quark bound states in analogy with QED.

The Hamiltonian of QCD in the Coulomb gauge can be given by

$$H = \frac{1}{2} \int d^3x (E_i^{\text{tr}2}(\vec{x}) + B_i^2(\vec{x})) + \frac{1}{2} \int d^3x d^3y (\rho(\vec{x}) \mathcal{V}(\vec{x}, \vec{y}) \rho(\vec{y})), \quad (1)$$

where E_i^{tr} , B_i , and ρ are the transverse electric field, the transverse magnetic field, and the color-charge density, respectively. The function \mathcal{V} in the second term is made by the Faddeev-Popov operator in the spatial direction, $M = -\vec{D} \vec{\partial} = -(\vec{\partial}^2 + g\vec{A} \times \vec{\partial})$,

$$\mathcal{V}(\vec{x}, \vec{y}) = \int d^3z \left[\frac{1}{M(\vec{x}, \vec{z})} (-\vec{\partial}_{(\vec{z})}^2) \frac{1}{M(\vec{z}, \vec{y})} \right]. \quad (2)$$

From the partition function with the Hamiltonian, Eq. (1), one can evaluate the time-time gluon propagator composed of the following two parts:

$$g^2 \langle A_0(x) A_0(y) \rangle = g^2 D_{00}(x-y) = V(x-y) + P(x-y), \quad (3)$$

where

$$V(x-y) = g^2 \langle \mathcal{V}(\vec{x}, \vec{y}) \rangle \delta(x_4 - y_4). \quad (4)$$

Equation (4) is the instantaneous color-Coulomb potential at equal time and causes antiscreening, so that this potential should be a confining potential to attract quarks in hadrons and is the most important quantity in the

Coulomb gauge confinement scenario. Note that Eq. (4), in the case of QED as a nonconfining theory, is identified as a Coulomb propagator $\langle -1/\partial_i^2 \rangle$ or a Coulomb potential $1/r$.

Simultaneously, Eq. (3) stands for a vacuum polarization,

$$P(x-y) = -g^2 \left\langle \int \mathcal{V}(\vec{x}, \vec{z}) \rho(\vec{z}, x_4) d^3z \times \int \mathcal{V}(\vec{y}, \vec{z}') \rho(\vec{z}', y_4) d^3z' \right\rangle, \quad (5)$$

which brings about the color-screening effect owing to the negative sign, producing the reduction of a color-confining force. Note that this term is associated with a quark-pair creation from vacuum when dynamical quarks exist. Consequently, we can consider that the instantaneous interaction is somewhat more classical than the time-dependent vacuum part.

B. Color-Coulomb instantaneous potential

One can define the color-dependent potentials on a lattice with the Polyakov line (PL) correlators [14]. In this study we separate the original potential obtained from the PL correlators into the color-Coulomb instantaneous and color vacuum polarization (retarded) parts with Coulomb gauge fixing. Moreover, the color-Coulomb potential defined by the link-link correlator, as will be described below, gives clear signals into practical numerical calculations even in the quenched lattice simulations.

We employ a partial-length Polyakov line (PPL), which can be defined as [22,23]

$$L(\vec{x}, T) = \prod_{t=1}^T U_0(\vec{x}, t), \quad T = 1, 2, \dots, N_t. \quad (6)$$

Here $U_0(\vec{x}, t) = \exp(iagA_0(\vec{x}, t))$ is an $SU(3)$ link variable in the temporal direction, and a , g , $A_0(\vec{x}, t)$, and N_t represent the lattice cutoff, the gauge coupling, the time component of a gauge potential, and the temporal-lattice size. A PPL correlator in the color-singlet channel is given by

$$G_1(R, T) = \frac{1}{3} \langle \text{Tr}[L(R, T) L^\dagger(0, T)] \rangle, \quad (7)$$

where R stands for $|\vec{x}|$. From Eq. (7) one evaluates a color-singlet potential on a lattice,

$$V(R, T) = \log \left[\frac{G_1(R, T)}{G_1(R, T+a)} \right]. \quad (8)$$

For the smallest temporal-lattice extension, i.e. $T = 0$, we define

$$V(R, 0) = -\log[G_1(R, 1)]. \quad (9)$$

Here $V(R, 0)$ in the Coulomb gauge is assumed to be the color-Coulomb instantaneous potential $V_{\text{coul}}(R)$. $V(R, T)$ in the limit $T \rightarrow \infty$ becomes the usual Polyakov line correlator. These two potentials are expected to satisfy

Zwanziger's inequality, $V_{\text{phys}}(R) \leq V_{\text{coul}}(R)$ [26], where $V_{\text{phys}}(R)$ is the physical potential extracted from the Wilson loop.

C. Color-dependent potentials on a lattice

We apply the above discussion to the other $SU(3)$ color-dependent potentials between two quarks [14]. A color-octet correlator on $q\bar{q}$ is given by

$$G_8(R, T) = \frac{1}{8} \langle \text{Tr} L(R, T) \text{Tr} L^\dagger(0, T) \rangle - \frac{1}{24} \langle \text{Tr} L(R, T) L^\dagger(0, T) \rangle, \quad (10)$$

and qq correlators in the symmetric-sextet and antisymmetric-triplet channels ($3 \otimes 3 = 6 \oplus \bar{3}$) are also given as

$$G_6(R, T) = \frac{3}{4} \langle \text{Tr} L(R, T) \text{Tr} L(0, T) \rangle + \frac{3}{4} \langle \text{Tr} L(R, T) L(0, T) \rangle, \quad (11)$$

$$G_{\bar{3}}(R, T) = \frac{3}{2} \langle \text{Tr} L(R, T) \text{Tr} L(0, T) \rangle - \frac{3}{2} \langle \text{Tr} L(R, T) L(0, T) \rangle. \quad (12)$$

In the same way as described in Eqs. (8) and (9), we obtain the color-dependent potentials in each color channel.

The above four potentials are classified in terms of the color (the quadratic Casimir) factor on the color- $SU(3)$ group in the fundamental representation:

$$C_{q\bar{q}}^1 = -\frac{4}{3}, \quad C_{q\bar{q}}^8 = \frac{1}{6}, \quad C_{qq}^{\bar{3}} = -\frac{2}{3}, \quad C_{qq}^6 = \frac{1}{3}, \quad (13)$$

for color-singlet, color-octet, color-triplet, and color-sextet channels, respectively. These coefficients appear as the proportional constant of the one-gluon-exchange potential.¹

D. Gauge fixing

Since the color-dependent potentials defined by the PPL correlators are not gauge invariant, we have to fix a gauge. We use the Coulomb gauge realized on a lattice as

$$\max_{\vec{x}} \sum_{i=1}^3 \text{Re Tr} U_i^\dagger(\vec{x}, t), \quad (14)$$

by repeating the following gauge rotations:

$$U_i(\vec{x}, t) \rightarrow U_i^\omega(\vec{x}, t) = \omega^\dagger(\vec{x}, t) U_i(\vec{x}, t) \omega(\vec{x} + \hat{i}, t), \quad (15)$$

where $\omega \in SU(3)$ is a gauge rotation matrix² and $U_i(\vec{x}, t)$

¹Here we intend to discuss an irreducible representation for the $q\bar{q}$ and qq sectors in relation to a so-called $\langle \lambda \cdot \lambda \rangle$ quark model. Therefore, in this study, we do not calculate the gauge-invariant Wilson-loop potentials in higher representations for the $q\bar{q}$ sector as introduced in Refs. [30–33].

²Here we used $\omega = e^{i\alpha \hat{\sigma}_i A_i}$, where the parameter α is chosen suitably depending on the lattice size, etc.

are spatial lattice link variables. The thermalized lattice configuration can be gauge fixed iteratively [34].

Because the Coulomb gauge fixing does not fully fix a gauge, one can still perform a time-dependent gauge rotation on the Coulomb gauge fixed links,

$$U_i(\vec{x}, t) \rightarrow \omega^\dagger(t) U_i(\vec{x}, t) \omega(t), \quad (16)$$

$$U_0(\vec{x}, t) \rightarrow \omega^\dagger(t) U_0(\vec{x}, t) \omega(t+1).$$

Therefore, $\text{Tr} L \text{Tr} L^\dagger$ and $\text{Tr} LL$ constructed by PPL are not invariant under this transformation equation (16). Accordingly, when performing numerical simulations for the octet and two qq correlators with $\text{Tr} L \text{Tr} L^\dagger$ and $\text{Tr} LL$, we should additionally implement a global temporal gauge fixing on the Coulomb gauge fixed links as

$$\max_{\vec{x}, t} \frac{1}{V} \sum_{\vec{x}, t} \text{Re Tr} U_0^\dagger(\vec{x}, t) \quad \text{under Eq. (16)}, \quad (17)$$

where $V = N_x N_y N_z$ is a spatial lattice volume. Note that this gauge fixing does not affect an intrinsic Coulomb gauge feature.

E. Infrared divergence of the color-dependent potential

In Coulomb gauge QCD, we find that infrared divergences cancel only for color-singlet interactions. Let us write the color-charge density for the two-quark system as $\rho_a \sim T_1^a \delta(x - x_0) + T_2^a \delta(x - y_0)$, where T_i^a are the generators of the color- $SU(3)$ group. The instantaneous potential with $R = x_0 - y_0$ [Eq. (2)] is given by

$$V(\vec{R}) = T_1^a T_2^b \int \frac{d\vec{p}}{(2\pi)^3} \frac{d^2(p)f(p)}{p^2} e^{i\vec{p} \cdot \vec{R}}, \quad (18)$$

where $d(p)$ is the expectation value of the Faddeev-Popov operator and $f(p)$ means the deviations of the factorization, e.g., $f(p) = 1$ if there is no quantum correction; this argument has been made in Refs. [35,36]. Here $T_1^a T_2^b$ is reduced to each color factor that appeared in Eq. (13). On the other hand, the self-energy interaction not depending on the distance R is written as

$$\Sigma = (T_i^a)^2 \int \frac{d\vec{p}}{(2\pi)^3} \frac{d^2(p)f(p)}{p^2}, \quad (19)$$

where the Casimir invariant $(T_i^a)^2 = 4/3$ in the fundamental representation of the $SU(3)$ group.

The infrared (not ultraviolet) divergence emerges in both Eqs. (18) and (19). If the term $d^2(p)f(p)$ behaves as $(1/\sqrt{p})^2 \cdot 1/p$, which would be responsible for the linear confinement $V \sim 1/p^4$, as has been analyzed in Refs. [36,37], then the infrared singularities unrelated to the linear potential arise from two terms:

$$V^{\text{IS}}(\vec{R}) = 4\pi (T_1^a T_2^b) \int_0^\infty dp \frac{1}{p^2}, \quad (20)$$

$$\Sigma^{\text{IS}} = 4\pi (T_i^a)^2 \int_0^\infty dp \frac{1}{p^2}.$$

Consequently, they are completely canceled in the case of the color-singlet representation since $(T_1^a T_2^b) + (T_i^a)^2 = (-4/3) + 4/3 = 0$. Meanwhile, the other cases are proportional to the following factors: $3/2, 2/3, 5/3$ for $8, 3^*,$ and 6 , respectively, implying that the color-sextet channel may diverge most strongly.

III. NUMERICAL RESULTS

A. Simulation parameters and statistics

We carry out $SU(3)$ lattice gauge simulations in the quenched approximation to calculate the color-decomposed PPL correlators. The lattice update is done by the heat-bath Monte Carlo algorithm with a plaquette Wilson gauge action. The lattice configuration numbers for the $18^4, 24^4,$ and 32^4 lattices are 600, 700, and 320; additionally, in order to investigate the volume dependence, we

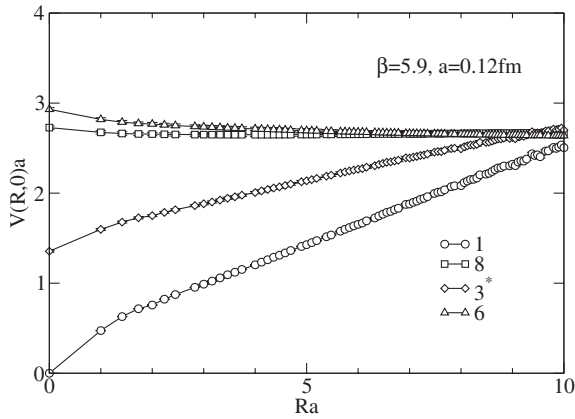


FIG. 1. Lattice numerical results of color-Coulomb instantaneous potentials between two quarks. ($\beta = 5.9, a \sim 0.12$ fm.)

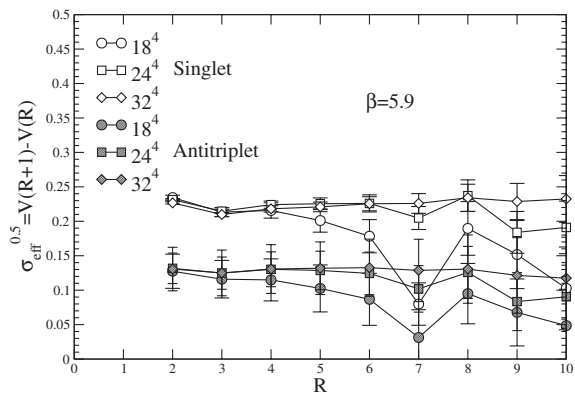


FIG. 2. Effective string tensions for the color-singlet and color-antitriplet channels in lattice units. Open (filled) symbols are the color-singlet (antitriplet) string tensions. Here the error bars are estimated in the error propagation. The effective string tensions at large R are strongly affected by the periodic boundary condition of a finite lattice; in contrast, owing to the increase of the lattice size, they become more stable even at large R .

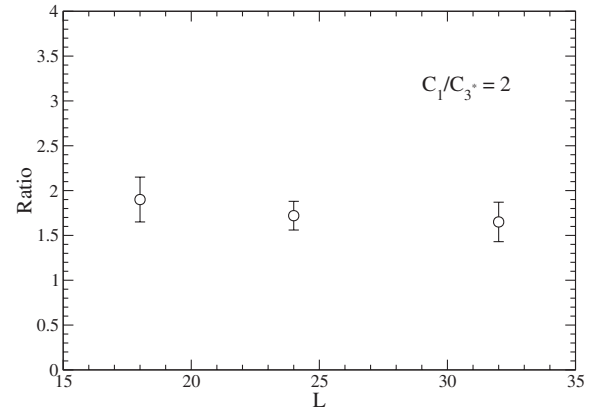


FIG. 3. The vertical axis stands for ratios K_1/K_{3^*} of the string tensions in the singlet and antitriplet channels, and the horizontal axis is the spatial lattice size.

added the 8^4 and 12^4 lattices with 200 configurations. The lattice coupling constant β for all the lattices is fixed to 5.9 corresponding to the lattice cutoff $a \sim 0.12$ fm [38].

B. Color-dependent potentials

Figure 1 shows numerical results for the color-Coulomb instantaneous potential $V(R, 0)$, in the color-singlet, color-octet, color-sextet, and color-triplet (antisymmetric) channels. We find that both the color singlet V_1 and color antitriplet V_{3^*} yield attractions at all distances, and, in particular, are linearly rising potentials at large distances. On the other hand, the color octet V_8 and color sextet V_6 potentials are repulsive forces, although the variation of these potentials on distances is small.

In order to investigate the magnitude of the string tensions, we calculate an effective string tension for the color-singlet and color-antitriplet channels. The confining potential can be described by the function $V(R) = C + KR + A/R$, where C is a self-energy constant term, K corresponds to the string tension, and the last term is the Coulomb term. Here the effective string tension is defined as $K = V(R+1) - V(R)$ in lattice units, which should be a constant for large quark separations if it is a confining potential with a finite string tension. In Fig. 2 we find that the K 's become stable over approximately $R = 3 \sim 4$ as the lattice size increases. When we use the data for $R = 3-6$ ($R = 3-5$ for the 18^4 lattice), we plotted in Fig. 3 the ratio K_1/K_{3^*} , which is found to be close to $C_1/C_{3^*} = 2$; for example, we obtain $K_1 = 0.218(2)$ and $K_{3^*} = 0.127(13)$ from the 24^4 lattice. Note that our definition of the color-Coulomb instantaneous part on a lattice in terms of the PPL correlator [Eq. (9)] does not completely exclude a vacuum polarization effect.³

³A possible way to improve this discussion may be to construct directly the instantaneous potential by the Faddeev-Popov propagator that has an infrared singularity [27,28].

For the color-octet and sextet channels, it is hard to discuss a precise value of both string tensions under the present statistical accuracy. In practice, from 24^4 lattice

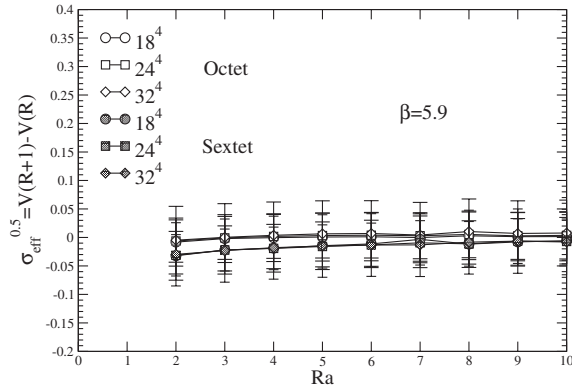


FIG. 4. Effective string tensions for the color-octet and color-sextet channels in lattice units.

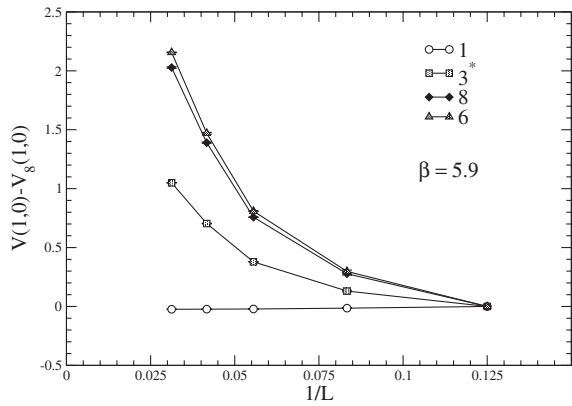


FIG. 5. Volume dependence of the color-dependent instantaneous potentials at the distance $R = 1$ scaled by $V_8^8(1,0)$ on the 8^4 lattice. The lattice sizes (L) used here are 8, 12, 18, 24, and 32. The variation of the singlet potential with the lattice volume is little while the other color-nonsinglet potentials diverge in the infinite volume limit.

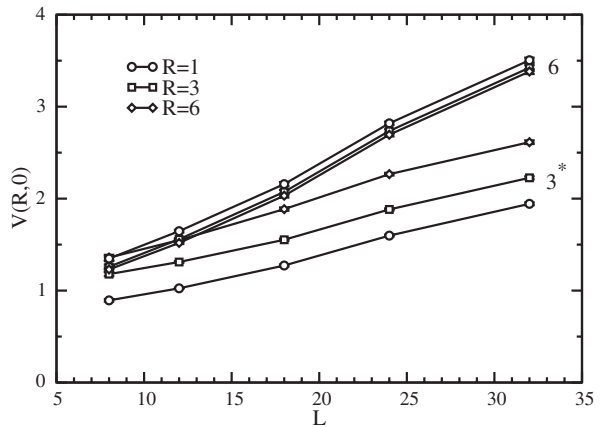
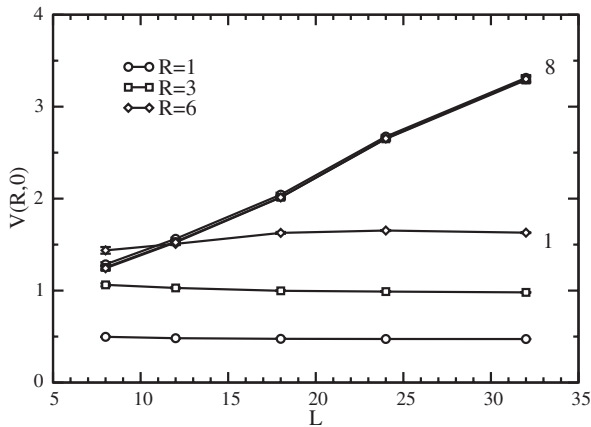


FIG. 6. Volume dependence of the color-dependent instantaneous potentials ($\beta = 5.9$) at the distances $R = 1, 3, 6$.

data and under the fitting range $R = 3-6$, we obtain the octet string tension $K_8 = 0.0014(222)$ and the sextet string tension $K_6 = -0.018(19)$, although the volume dependence does not appear large, as shown in Fig. 4. This indicates that the long-range behavior of the octet and sextet channels is quantitatively a minor contribution to the two-quark system. However, in order to work out a more quantitative measurement for the repulsive channels (and also the attractive channels), one may need enough statistics on a larger lattice.

C. Divergence of color-nonsinglet potentials

Here we consider the infrared divergence property of the color-dependent potentials while the string tensions obtained from them have little volume dependence, as shown in the previous section. The short-distance Coulomb term $\sim 1/R$, which is not related to the color confinement, may not matter in this argument. Figure 5 shows our nonperturbative numerical results, by which we find that the color-singlet potential has little volume dependence and the absolute value of the color-nonsinglet potentials increases with the lattice volume; this tendency remains at the distances $R = 3$ and 6, as displayed in Fig. 6. Therefore, we conclude that the color-nonsinglet potentials diverge regardless of the distance.

Moreover, in order to estimate the degree of divergence for the color-nonsinglet channels, we assume the fitting function $f(R) = C + KR$ for the potential data in the distance $R = 3-6$ (long range). The corresponding self-energy terms C fitted well are plotted in Fig. 7; this graph shows that the divergence contribution increases monotonically with the volume. Therefore we adopt the linear function $y = Dx + d$, where D may correspond to the constant meaning the degree of divergence. The fitted results are summarized in Table I, which gives the conclusion that the magnitude of the divergence on the finite lattice depends on the ratio being 4:9:10 for 3^* , 8, and 6 as observed in Sec. II E. However, note that they will diverge

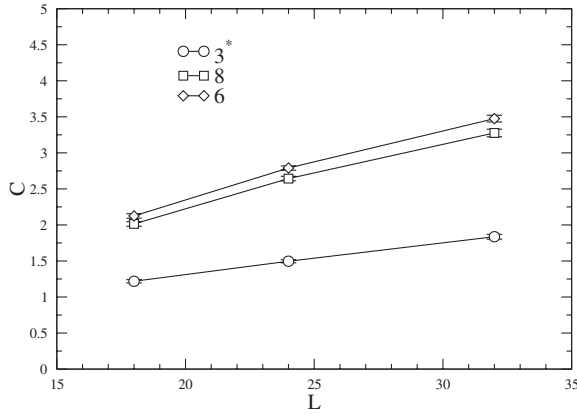


FIG. 7. Volume dependence of the self-energy term for color-nonsinglet potentials. The self-energy term diverges in the infinite volume limit.

TABLE I. Table of fitting results to estimate the degree of divergence in color-nonsinglet channels. $y = Dx + d$ is assumed as a fitting function to fit the data of Fig. 7.

	3*	8	6
D	0.044(06)	0.092(14)	0.098(14)
d	0.42(07)	0.38(10)	0.39(10)
χ^2/ndf	0.19	4.20	4.63

equally to infinity in the large volume limit, as shown in Figs. 5 and 7. This indicates that the color-nonsinglet quarks cannot exist independently; finally, they will become a color-singlet state with finite energy to compensate insufficient color degrees of freedom.

This numerical result does not contradict the dual-Ginzburg-Landau picture, in which one understands that the color-singlet flux between two quarks is shrunk like a string while the color-nonsinglet flux will radiate rather than produce a closed string. A singularity of the color flux not making the closed string can be expected to emerge as the volume dependence on the lattice gauge theory.

IV. SUMMARY

We have studied the long-distance color-dependent forces between two quarks in the quenched $SU(3)$ lattice simulation with the Polyakov line correlator. Here we focus on the color-Coulomb instantaneous term in Coulomb gauge QCD, which has been discussed in the Gribov-Zwanziger confinement scenario and is required to make the hadron bound state consisting of quarks.

Our numerical simulation shows that the color-singlet $q\bar{q}$ channel as well as the color-antitriplet qq (diquark) channel causes a linearly confining potential at large distances. The other color-octet and color-sextet channels at large distances also yield repulsive forces. In addition, we find that the string tensions in the color-singlet and color-

antitriplet channels do not have significant volume dependence.

We also investigated the infrared divergence of color-nonsinglet potentials and found that the divergence on the finite lattice seems to be proportional to the color (Casimir) factor; however, the divergence of the color-singlet channel is not left over. In the infinite volume limit the color-dependent potentials except the color-singlet channel will diverge; in particular, the color-sextet channel diverges most strongly as expected. This conclusion is consistent with the dual-Ginzburg-Landau picture of the color confinement.

This approach, in which we take notice of the color-Coulomb instantaneous part, may be suitable for further work to investigate three-quark color-dependent forces for the understanding of baryons as well as new multi-quark particles. It is also necessary to study how the vacuum polarization term affects the instantaneous forces, because it is reported in Refs. [13,39] that the octet (adjoint) channel calculated by the full-length Polyakov line correlator with the vacuum polarization gives the complicated distance dependence at large distances.

ACKNOWLEDGMENTS

The simulation was performed on SX-5 and SX-8 (NEC) vector-parallel computers at the RCNP of Osaka University. We appreciate the warm hospitality and support of the RCNP administrators.

APPENDIX

In Eq. (18), if the Coulomb kernel $K(p)$ produces a confining force, it is reported in Ref. [37] that the ghost factor $d(p)$ and the Laplacian factor $f(p)$ behave approximately as $1/\sqrt{p}$ and $1/p$, respectively. Thus we assume that $K(p)$ is $1/p^2$. Omitting the $T_1^a T_2^b$ term, one also calculates Eq. (18):

$$\begin{aligned}
 V(\vec{R}) &= \int \frac{d\vec{p}}{(2\pi)^3} \frac{K(p)}{p^2} e^{i\vec{p}\vec{R}} \\
 &= \int_0^{2\pi} \int_{-1}^1 d\cos\theta \int_0^\infty p^2 dp \theta \frac{K(p)}{p^2} e^{ipR\cos\theta} \\
 &= \frac{2\pi}{iR} \int_0^\infty dp \frac{K(p)}{p} (e^{ipR} - e^{-ipR}) \\
 &= \frac{2\pi}{iR} \int_{-\infty}^\infty dp \frac{K(p)}{p} e^{ipR} \\
 &= \frac{2\pi}{iR} \int_{-\infty}^\infty dp \frac{K(p)}{p} \left(1 + ipR + \frac{1}{2}(ipR)^2 \right. \\
 &\quad \left. + \frac{1}{3}(ipR)^3 + \dots \right). \tag{A1}
 \end{aligned}$$

Here we perform the Taylor expansion in the infrared limit $p = 0$ for e^{ipR} . In the above equation, the first term disappears because it is an odd function on p ; the second term

proportional to $1/p^2$ causes the infrared divergence; the third term produces a (linear) potential; and the other terms are irrelevant. Finally, the second term relating to the divergence is

$$V^{\text{IS}}(\vec{R}) = 2\pi(T_1^a T_2^b) \int_{-\infty}^{\infty} dp \frac{1}{p^2} = 4\pi(T_1^a T_2^b) \int_0^{\infty} dp \frac{1}{p^2}. \quad (\text{A2})$$

In the same way, the relevant contribution from the self-energy of Eq. (19) is also given by

$$\Sigma^{\text{IS}} = 4\pi(T_i^a)^2 \int_0^{\infty} dp \frac{1}{p^2}. \quad (\text{A3})$$

-
- [1] T. Nakano *et al.* (LEPS Collaboration), Phys. Rev. Lett. **91**, 012002 (2003).
- [2] E. S. Swanson, Phys. Rep. **429**, 243 (2006).
- [3] G. S. Bali, Phys. Rep. **343**, 1 (2001).
- [4] E. Braaten and S. Fleming, Phys. Rev. Lett. **74**, 3327 (1995); E. Braaten and Y. Q. Chen, Phys. Rev. Lett. **76**, 730 (1996); M. Cacciari and M. Krämer, Phys. Rev. Lett. **76**, 4128 (1996).
- [5] R. A Briere *et al.* (CLEO Collaboration), Phys. Rev. D **70**, 072001 (2004).
- [6] G. T. Bodwin, J. Lee, and D. K. Sinclair, Phys. Rev. D **72**, 014009 (2005).
- [7] M. Anselmino, E. Predazzi, S. Ekelin, S. Fredriksson, and D. B. Lichtenberg, Rev. Mod. Phys. **65**, 1199 (1993).
- [8] R. Jaffe and F. Wilczek, Phys. Rev. Lett. **91**, 232003 (2003).
- [9] K. Nagata, A. Hosaka, and L. J. Abu-Raddad, Phys. Rev. C **72**, 035208 (2005).
- [10] K. Nagata and A. Hosaka, J. Phys. G **32**, 777 (2006).
- [11] L. J. Abu-Raddad, A. Hosaka, D. Ebert, and H. Toki, Phys. Rev. C **66**, 025206 (2002).
- [12] K. Nagata and A. Hosaka, Prog. Theor. Phys. **111**, 857 (2004).
- [13] A. Nakamura and T. Saito, Phys. Lett. B **621**, 171 (2005).
- [14] S. Nadkarni, Phys. Rev. D **33**, 3738 (1986); **34**, 3904 (1986).
- [15] A. Nakamura and T. Saito, Prog. Theor. Phys. **112**, 183 (2004).
- [16] A. Nakamura and T. Saito, Prog. Theor. Phys. **111**, 733 (2004).
- [17] Y. Maezawa, N. Ukita, S. Aoki, S. Ejiri, T. Hatsuda, N. Ishii, and K. Kanaya, Phys. Rev. D **75**, 074501 (2007).
- [18] M. Döring, K. Hübner, O. Kaczmarek, and F. Karsch, Phys. Rev. D **75**, 054504 (2007).
- [19] D. Zwanziger, Nucl. Phys. **B518**, 237 (1998).
- [20] L. Baulieu and D. Zwanziger, Nucl. Phys. **B548**, 527 (1999).
- [21] A. Niégawa, Phys. Rev. D **74**, 045021 (2006); A. Niégawa, M. Inui, and H. Kohyama, Phys. Rev. D **74**, 105016 (2006).
- [22] J. Greensite and Š. Olejník, Phys. Rev. D **67**, 094503 (2003).
- [23] J. Greensite, Š. Olejník, and D. Zwanziger, Phys. Rev. D **69**, 074506 (2004).
- [24] A. Nakamura and T. Saito, Prog. Theor. Phys. **115**, 189 (2006).
- [25] Y. Nakagawa, A. Nakamura, T. Saito, H. Toki, and D. Zwanziger, Phys. Rev. D **73**, 094504 (2006).
- [26] D. Zwanziger, Phys. Rev. Lett. **90**, 102001 (2003).
- [27] J. Greensite, Š. Olejník, and D. Zwanziger, J. High Energy Phys. **05** (2005) 070.
- [28] Y. Nakagawa, A. Nakamura, T. Saito, and H. Toki, Phys. Rev. D **75**, 014508 (2007).
- [29] A. P. Szczepaniak and E. S. Swanson, Phys. Rev. D **65**, 025012 (2001).
- [30] S. Deldar, Phys. Rev. D **62**, 034509 (2000).
- [31] G. S. Bali, Phys. Rev. D **62**, 114503 (2000).
- [32] M. Faber, J. Greensite, and Š. Olejník, Phys. Rev. D **57**, 2603 (1998).
- [33] Y. Koma, E.-M. Ilgenfritz, H. Toki, and T. Suzuki, Phys. Rev. D **64**, 011501(R) (2001).
- [34] J. E. Mandula and M. Ogilvie, Phys. Lett. B **185**, 127 (1987).
- [35] D. Zwanziger, Nucl. Phys. **B485**, 185 (1997).
- [36] P. O. Bowman and A. P. Szczepaniak, Phys. Rev. D **70**, 016002 (2004).
- [37] K. Langfeld and L. Moyaerts, Phys. Rev. D **70**, 074507 (2004).
- [38] K. Akemi *et al.* (QCDTARO Collaboration), Phys. Rev. Lett. **71**, 3063 (1993).
- [39] O. Philipsen, Phys. Lett. B **535**, 138 (2002).